Steric influence of the 6-methyl group on the molecular and crystal structures of copper(II) chloride complexes with 2-(N-acetylamino)-6-methylpyridine

Anton I. Smolentsev [a,b,*], Elisaveta V. Lider [a,b], Ludmila G. Lavrenova [a,b], Liliya A. Sheludyakova [a], Artem S. Bogomyakov [c], Sergei F. Vasilevsky [b,d]

[a] Nikolaev Institute of Inorganic Chemistry, Siberian Branch of the Russian Academy of Sciences, 3, Acad. Lavrentiev Ave., 630090 Novosibirsk, Russia
[b] Novosibirsk State University, 2, Pirogova Str., 630090 Novosibirsk, Russia
[c] International Tomography Center, Siberian Branch of the Russian Academy of Sciences, 3a, Institutskaya Str., 630090 Novosibirsk, Russia
[d] Institute of Chemical Kinetics and Combustion, Siberian Branch of the Russian Academy of Sciences, 3, Institutskaya Str., 630090 Novosibirsk, Russia

ARTICLE INFO

ABSTRACT

New coordination compounds of copper(II) chloride with 2-(N-acetylamino)-6-methylpyridine (L) of the compositions $[Cu_2L_2Cl_4]$ (**1**), $[CuL(H_2O)Cl_2]\cdot L$ (**1a**), and $[CuL_2Cl][CuLCl_3]\cdot C_2H_5OH$ (**2**) have been prepared by the reactions between ethanol solutions of L and ethanol solutions of $CuCl_2\cdot 2H_2O$ at different Cu:L ratios. The compounds have been characterized by a set of methods including elemental analysis, IR-spectroscopy, single-crystal X-ray diffraction analysis, and magnetic susceptibility measurements in the range 5–300 K (for **1**). The crystal structures of **1** and **1a** revealed distorted square-pyramidal geometry around Cu(II) centers, while in **2** both distorted square-pyramidal and trigonal–bipyramidal coordinations are present. L acts as a bidentate chelate ligand bound to the metal center through the pyridine N atom and the acetyl O atom. The results of the study demonstrate that the presence of 6-methyl substituent in L provides a high steric hindrance, precluding the formation of complexes with a distorted octahedral coordination of Cu(II).

© 2014 Elsevier Ltd. All rights reserved.

1. Introduction

The pyridine derivatives are widely used in the practical applications. These compounds are known as important substrates for the preparation of high-effective plants growth regulators; moreover, they are good complexing agents for the extraction of metal ions from waste water. The constant interest to the pyridine derivatives can also be explained by the fact that many of them, natural and synthetic, display significant physiological activity. A special place in the chemistry of pyridine is occupied by 2-(N-acylamino)pyridines. The research in this field can be exemplified by many works, including [1] focused on the elucidation of influence of some 2-(N-acylamino)pyridines on the growth and division of cells. It is noteworthy that just the simplest member, unsubstituted 2-(N-acetylamino)pyridine, was found to be the most active

anticancer agent. Besides, a number of 2-(N-acylamino)pyridine ligands and their Ni(II) complexes were found to be suitable catalysts for the ethylene oligomerization [2]. The perspectives of use of 2-(N-acylamino)pyridine derivatives for the design of new asymmetric binuclear metal complexes were demonstrated recently [3].

It is known that the molecule of 2-(N-acylamino)pyridine has one Lewis-acidic (NH group) and two Lewis-basic (pyridine N atom and carbonyl O atom) coordination sites. The introduction of alkyl substituents in the heterocycle affects electron density that can be used to modify the donor properties of the ligand. On the other hand, the presence of substituents in the α-position of the pyridine ring can create a steric hindrance that blocks ligand access to the metal ion, significantly changing the coordination geometry. Particularly, 2-(N-acylamino)pyridines, including their 6-methyl derivatives, were used as convenient model compounds for the investigation of steric influence of the alkyl groups on molecular self-association in the solid state and in solution [4]. At the same time, the structural data on the transition metal complexes with simple (having only small acyl groups) 2-(N-acylamino)pyridines are very limited. In one of the earliest work in this field [5], several

* Corresponding author at: Nikolaev Institute of Inorganic Chemistry, Siberian Branch of the Russian Academy of Sciences, 3, Acad. Lavrentiev Ave., 630090 Novosibirsk, Russia. Tel.: +7 383 330 9466; fax: +7 383 330 9489.
E-mail addresses: smolentsev@ngs.ru (A.I. Smolentsev), lisalider@ngs.ru (E.V. Lider).

complexes of Pd(II), Co(II), Ni(II), and Cu(II) with 2-(N-acetyl-amino)pyridine were synthesized, but no attempts were made to characterize them by X-ray diffraction methods. Some lanthanide complexes with 2-(N-acetylamino)-4-methylpyridine were investigated spectroscopically [6]. To date, structural data are available for the complexes of Ni(II), Zn(II) [7], Cu(II) [8], and Hg(II) [9] with 2-(N-acetylamino)pyridine, Cu(II) complex with 2-(N-acetyl-amino)-4-methylpyridine [10], and Rh(II) complex with 2-(N-ace-tylamino)-6-methylpyridine [11]. In view of this, it was of interest to prepare a representative series of transition metal complexes with sterically active 2-(N-acetylamino)-6-methylpyridine, and to evaluate relationships between molecular and crystal structures formed under steric influence of the α-substituted heterocycle.

Thus, in this paper, we report the synthesis and characterization of three complexes of Cu(II) chloride with 2-(N-acetylamino)-6-methylpyridine (L), the full formulas of which are $[Cu_2L_2Cl_4]$ (**1**), $[CuL(H_2O)Cl_2] \cdot L$ (**1a**), and $[CuL_2Cl][CuLCl_3] \cdot C_2H_5OH$ (**2**).

2. Experimental

2.1. Materials and instruments

$CuCl_2 \cdot 2H_2O$ used for the synthesis of the title compounds was of 'pure for analysis' quality. All other reagents and solvents used were commercially available products of reagent grade quality. IR spectra of the complexes were recorded on Scimitar FTS 2000 and Vertex 80 spectrometers in the range of 4000–100 cm^{-1}. The samples were prepared as mineral and fluorinated oil mulls and polyethylene pellets. The metal content of the compounds synthesized was determined by complexonometry after the samples were decomposed in a mixture of concentrated H_2SO_4 and $HClO_4$ (1:2). Elemental analyses of C, H, and N were performed using a Euro EA 3000 analyzer using a standard procedure. All the compounds show satisfactory elemental analyses (Table 1) and exhibit well-resolved sharp IR bands confirming their purity.

2.2. Synthesis of L

The synthetic procedure for the preparation of L is similar to that reported previously [4] and [12]. However, it involves some changes and adaptations and deserves to be described herein.

Solution of acetyl chloride (1.305 g, 16.5 mmol) in dry toluene (30 mL) was added dropwise to the magnetically stirred mixture of 2-amino-6-methylpyridine (1.62 g, 15 mmol) and triethylamine (1.65 g, 16.5 mmol) in dry toluene (15 mL) at 5 °C. The reaction mixture was allowed to reach room temperature and stirred for 2 h. To the reaction mixture, water (30 mL) was added, organic layer was separated. The water layer was extracted once with methylene chloride (20 mL), and the combined organic layers were dried over Na_2SO_4, the solvent was evaporated at reduced pressure. Recrystallization of crude product from hexane/ethyl acetate (8:1 v/v) mixture gave 2.1 g (93%) of 2-(N-acethylamino)-6-methylpyr-idine with m.p. 87–88 °C (lit. m.p. 91–92 °C [4] or 85–88 °C [12]).

2.3. Synthesis of $[Cu_2L_2Cl_4]$ (**1**)

L (0.30 g, 2 mmol) was dissolved in 5 mL of hot ethanol and added to 5 mL of hot ethanol solution of $CuCl_2 \cdot 2H_2O$ (0.34 g, 2 mmol). After evaporation of the excess of solvent up to one-third of its original volume and cooling the solution in an ice bath, in about an hour a light brown precipitate of **1** was formed. The precipitate was filtered off, washed twice with ethanol, and dried in

Table 1
Elemental analysis results for L and complexes **1** and **2** (%).

Results	L, $C_8H_{10}N_2O$	**1**, $C_{16}H_{20}Cl_4Cu_2N_4O_2$	**2**, $C_{26}H_{36}Cl_4Cu_2N_6O_4$
C calcd.	64.0	33.3	41.5
Found	64.0	33.8	40.8
H calcd.	6.7	3.6	4.9
Found	6.7	3.5	4.7
N calcd.	18.4	9.6	11.0
Found	18.6	9.8	11.0
Cu calcd.	–	22.0	16.3
Found	–	22.3	16.6

Table 2
Crystal data and structure refinement details for **1**, **1a**, and **2**.

Compound	**1**	**1a**	**2**
Empirical formula	$C_{16}H_{20}Cl_4Cu_2N_4O_2$	$C_{16}H_{22}Cl_2CuN_4O_3$	$C_{26}H_{36}Cl_4Cu_2N_6O_4$
Formula weight	569.24	452.82	765.49
T (K)	296(2)	150(2)	296(2)
Crystal size (mm)	$0.20 \times 0.15 \times 0.04$	$0.30 \times 0.20 \times 0.12$	$0.20 \times 0.13 \times 0.02$
Crystal system	triclinic	monoclinic	monoclinic
Space group	$P\bar{1}$	$P2_1/n$	$P2_1/c$
Z	1	4	4
a (Å)	7.5466(6)	7.4859(3)	7.8125(3)
b (Å)	8.9629(7)	32.8133(17)	29.2690(8)
c (Å)	9.7100(8)	8.4818(4)	14.5631(3)
α (°)	106.033(3)		
β (°)	107.404(3)	111.1300(10)	94.5200(10)
γ (°)	103.783(3)		
V (Å^3)	564.27(8)	1943.36(16)	3319.70(17)
D_{calc} (g cm^{-3})	1.675	1.548	1.532
μ (Mo Kα) (mm^{-1})	2.377	1.422	1.644
θ Range (°)	2.52–27.52	2.48–27.50	1.98–27.52
h, k, l indices range	$-9 \leqslant h \leqslant 9, -11 \leqslant k \leqslant 11, -11 \leqslant l \leqslant 12$	$-6 \leqslant h \leqslant 9, -42 \leqslant k \leqslant 42, -11 \leqslant l \leqslant 10$	$-7 \leqslant h \leqslant 10, -38 \leqslant k \leqslant 38, -17 \leqslant l \leqslant 18$
$F(000)$	286	932	1568
Reflections collected	5742	11776	22767
Unique reflections (R_{int})	2589 (0.0198)	4436 (0.0482)	7373 (0.0522)
Observed reflections	2334 $[I > 2\sigma(I)]$	3873 $[I > 2\sigma(I)]$	4727 $[I > 2\sigma(I)]$
Parameters refined	129	247	387
$R[F^2 > 2\sigma(F^2)]$	$R_1 = 0.0249, wR_2 = 0.0659$	$R_1 = 0.0593, R_2 = 0.1071$	$R_1 = 0.0428, R_2 = 0.0855$
$R(F^2)$ (all data)	$R_1 = 0.0288, R_2 = 0.0676$	$R_1 = 0.0701, wR_2 = 0.1112$	$R_1 = 0.0861, R_2 = 0.0949$
GOOF on F^2	1.045	1.183	0.959
$\Delta\rho_{max}, \Delta\rho_{min}$ (e Å^{-3})	0.625, −0.224	0.654, −0.557	0.483, −0.368

air. Yield: 0.42 g (70%). For the X-ray diffraction study, single crystals (brown plates) of 1 were obtained by slow crystallization during a few days from ethanol solution (10 mL) of 1 mmol of CuCl$_2$·2H$_2$O (0.17 g) and 1 mmol of L (0.15 g) at room temperature.

As a by-product, single crystals (green–blue plates) of the complex [CuL(H$_2$O)Cl$_2$]·L (1a) suitable for X-ray diffraction analysis were obtained by slow crystallization from the mother liquor after separation of the bulk of 1. Due to the lack of crystals of 1a, no analyses were performed except for X-ray diffraction. The yield of 1a could not be given by the same reason.

2.4. Synthesis of [CuL$_2$Cl][CuLCl$_3$]·C$_2$H$_5$OH (2)

CuCl$_2$·2H$_2$O (0.08 g, 0.5 mmol) was dissolved in 5 mL of ethanol and added to 5 mL of ethanol solution of L (0.15 g, 1 mmol) at room temperature with magnetic stirring. After a few days, the green plates were filtered off, washed twice with ethanol, and dried in air. Yield: 0.17 g (60%).

2.5. X-ray crystallography

The single crystals of compounds 1, 1a and 2 were selected directly from the mother liquors and mounted on glass fibers using epoxy resin. Single-crystal X-ray diffraction data were collected on a Bruker-Nonius X8 APEX CCD diffractometer (graphite monochromatized Mo Kα radiation, $\lambda = 0.71073$ Å, φ and ω scans of narrow frames) equipped with a 4 K CCD area detector at 150(2) K for 1a and 296(2) K for 1 and 2. Absorption corrections were applied using the SADABS program [13]. The crystal structures were solved by direct methods and were refined by full-matrix least-squares techniques with the use of the SHELXTL package [13]. Molecular graphics was performed using standard means of SHELXTL package and DIAMOND program [14]. All non-hydrogen atoms were refined anisotropically. Hydrogen atoms of the water molecule in 1a were found in the difference Fourier maps and refined isotropically with O–H and H···H distances restrained (using DFIX and DANG instructions) to 0.82(2) and 1.30(2) Å, respectively. Hydrogen atoms of the 2-(N-acetylamino)-6-methylpyridine ligands were placed in geometrically calculated positions and treated as riding on their parent atoms. Crystallographic data as well as details of data collection and refinement for complexes 1, 1a and 2 are given in Table 2. Selected bond distances and angles are given in Table 3.

2.6. Magnetic susceptibility measurements

The magnetic susceptibility of the polycrystalline sample of dimeric complex 1 was measured with a Quantum Design MPMSXL SQUID magnetometer in the temperature range 5–300 K with magnetic field of up to 5 kOe. The complex showed no any field dependence of molar magnetization at low temperatures. Diamagnetic corrections were made using the Pascal constants. The effective magnetic moment was calculated as $\mu_{eff}(T) = [(3 k/N_A\mu_B^2)\chi T]^{1/2} \approx (8\chi T)^{1/2}$.

3. Results and discussion

3.1. Synthesis

2-(N-Acetylamino)-6-methylpyridine (L) was prepared in good yield through the condensation reaction of 2-amino-6-methylpyridine and acetyl chloride according to a modified procedure [4] (Scheme 1). The reaction was smoothly performed in dry toluene at room temperature. The resulting mixture was quenched with water and filtered. The white solid was thoroughly washed with methylene chloride and dried at reduced pressure. The

Table 3
Selected bond lengths (Å) and angles (°) around the Cu^{2+} ion in 1, 1a, and 2.

| Bond/angle	1a	1	2, cation	2, anion
Cu(1)–N(1)	2.006(3)	2.0038(15)	2.015(2)	–
Cu(1)–N(3)	–	–	2.019(2)	–
Cu(2)–N(5)	–	–	–	2.029(3)
Cu(1)–O(1)	2.112(2)	2.1228(15)	2.051(2)	–
Cu(1)–O(2)	–	–	2.080(3)	–
Cu(2)–O(3)	–	–	–	2.158(2)
Cu(1)–O(1W)	1.957(3)	–	–	–
Cu(1)–Cl(1)	2.3629(10)	2.2809(6)	2.2580(11)	–
Cu(1)–Cl(2)	2.2794(10)	2.2814(5)	–	–
Cu(1)–Cl(2)^i	–	2.3677(6)	–	–
Cu(2)–Cl(2)	–	–	–	2.3755(10)
Cu(2)–Cl(3)	–	–	–	2.2448(11)
Cu(2)–Cl(4)	–	–	–	2.2972(10)
N(1)–Cu(1)–O(1)	90.39(11)	90.98(6)	86.58(9)	–
N(1)–Cu(1)–O(2)	–	–	95.26(10)	–
N(3)–Cu(1)–O(1)	–	–	89.26(9)	–
N(3)–Cu(1)–O(2)	–	–	87.76(10)	–
N(5)–Cu(2)–O(3)	–	–	–	88.32(10)
N(1)–Cu(1)–N(3)	–	–	174.80(11)	–
N(1)–Cu(1)–O(1W)	178.01(13)	–	–	–
N(1)–Cu(1)–Cl(1)	92.57(9)	93.24(5)	91.84(9)	–
N(1)–Cu(1)–Cl(2)	89.49(8)	166.77(5)	–	–
N(1)–Cu(1)–Cl(2)^i	–	86.72(5)	–	–
N(3)–Cu(1)–Cl(1)	–	–	89.93(8)	–
N(5)–Cu(2)–Cl(2)	–	–	–	88.86(8)
N(5)–Cu(2)–Cl(3)	–	–	–	171.50(8)
N(5)–Cu(2)–Cl(4)	–	–	–	87.39(8)
O(1)–Cu(1)–Cl(1)	93.45(8)	96.53(5)	146.74(8)	–
O(1)–Cu(1)–Cl(2)	108.91(8)	99.92(4)	–	–
O(1)–Cu(1)–Cl(2)^i	–	95.93(5)	–	–
O(2)–Cu(1)–Cl(1)	–	–	124.33(8)	–
O(3)–Cu(2)–Cl(2)	–	–	–	90.88(7)
O(3)–Cu(2)–Cl(3)	–	–	–	100.13(8)
O(3)–Cu(2)–Cl(4)	–	–	–	100.75(8)
O(1)–Cu(1)–O(2)	–	–	88.86(11)	–
O(1W)–Cu(1)–Cl(1)	86.24(10)	–	–	–
O(1W)–Cu(1)–Cl(2)	91.01(9)	–	–	–
O(1)–Cu(1)–O(1W)	91.27(12)	–	–	–
Cl(1)–Cu(1)–Cl(2)	157.54(4)	92.94(2)	–	–
Cl(1)–Cu(1)–Cl(2)^i	–	167.54(2)	–	–
Cl(2)–Cu(1)–Cl(2)^i	–	84.73(2)	–	–
Cl(2)–Cu(2)–Cl(3)	–	–	–	90.08(4)
Cl(2)–Cu(2)–Cl(4)	–	–	–	167.67(4)
Cl(3)–Cu(2)–Cl(4)	–	–	–	91.89(4)

Symmetry code: (i) $1 - x$, $1 - y$, $1 - z$.
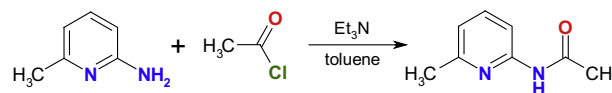
Scheme 1. Synthesis of L.

product was recrystallized from the hexane/ethyl acetate mixture. Elemental analysis showed that the ligand was of enough purity to be used in subsequent reactions.

The title copper(II) chloride complexes with 2-(N-acethylamino)-6-methylpyridine (L) were obtained by the reactions between ethanol solutions of CuCl$_2$·2H$_2$O and L at Cu:L ratios of 1:1 and 1:2, as shown in the Scheme 2.

The reaction performed with the initial Cu:L ratio of 1:1 and followed by immediate evaporation of the excess solvent yielded the compound 1 in the form of a polycrystalline precipitate. Scarce crystals of 1a appeared on standing for a week of the mother liquor left after precipitation of the bulk of 1. The reaction performed with the same Cu:L ratio, but followed by slow (several days) crystallization at room temperature yielded brown plate crystals of the binuclear complex 1, in which each Cu^{2+} ion is bidentately coordi-
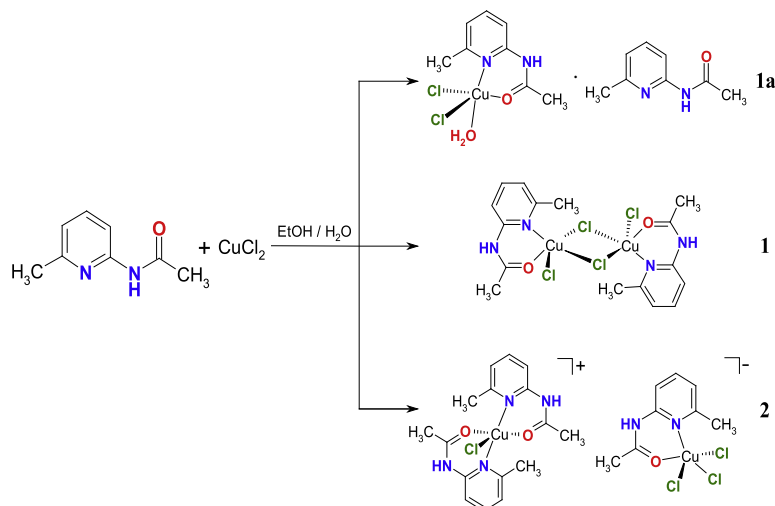
Scheme 2. Synthesis of the complexes **1**, **1a** and **2**.

nated by L and also bears one terminal and two bridging chloride ions (CuNOCl$_3$ coordination unit). Coordination unit of the complex **1a**, CuNO$_2$Cl$_2$, includes one bidentate ligand L, one water molecule, and two chloride ions, each coordinated to the Cu^{2+} ion. Finally, the combination of Cu:L = 1:2 stoichiometry and slow crystallization of the resulting solution led to the formation of the double complex salt **2**. The cationic part of **2** consists of the Cu^{2+} ion bidentately coordinated by two L molecules and one chloride ion (CuN$_2$O$_2$Cl coordination unit). The anionic part of **2** includes the Cu^{2+} ion coordinated by one L molecule and three chloride ions; coordination unit CuNOCl$_3$. The nontrivial composition of **2** most likely indicates the competition between ligands having a comparably strong metal-coordination ability. On the other hand, the presence of the 6-methyl group on the pyridine ring of L presumably prevents the formation of the complexes *trans*-[CuL$_2$Cl$_2$], which were reported previously for both unsubstituted 2-(N-acetylamino)pyridine and its 4-methyl derivative. By this reason, at the Cu:L = 1:2 ratio the common distorted octahedral coordination with two nearly coplanar L ligands is not possible; it rearranges into a trigonal bipyramid with large (>50°) dihedral angles between the ligand planes. Thus, although the cationic part of **2** includes two L molecules per metal ion (i.e. the 1:2 stoichiometry is formally met), the overall Cu:L ratio in the entire complex is lower, being 1:1.5, which can be attributed to the steric hindrance provided by the 6-methyl group.

3.2. Description of crystal structures

The crystals of compound **1** are triclinic; space group *P*–1 and the unit cell contains 1 formula unit. The asymmetric unit consists only half of the binuclear complex [Cu$_2$L$_2$Cl$_4$] with all atoms occupying general positions. The entire [Cu$_2$L$_2$Cl$_4$] molecule is generated by the inversion center located at (1/2, 1/2, 1/2). The coordination environment of the Cu^{2+} ion includes N and O atoms of the bidentate ligand L, and three chloride ions, two of which are μ2-bridging (Fig. 1). These atoms form a distorted tetragonal pyramid with the basal plane defined by N(1), Cl(1), Cl(2), and symmetry-generated Cl(2)^i atoms ((i): 1 – *x*, 1 – *y*, 1 – *z*). The Cu–N and Cu–O distances are 2.0038(15) and 2.1228(15) Å, respectively. Three Cu–Cl bond lengths are 2.2809(6), 2.2814(5) and 2.3677(6) Å; there is no clear dependence on the coordination mode of the particular chloride ion. The Cu···Cu separation within the binuclear unit is 3.4356(5) Å. Each binuclear unit is further connected to two adjacent units through pairs of N$_{amide}$–H···Cl

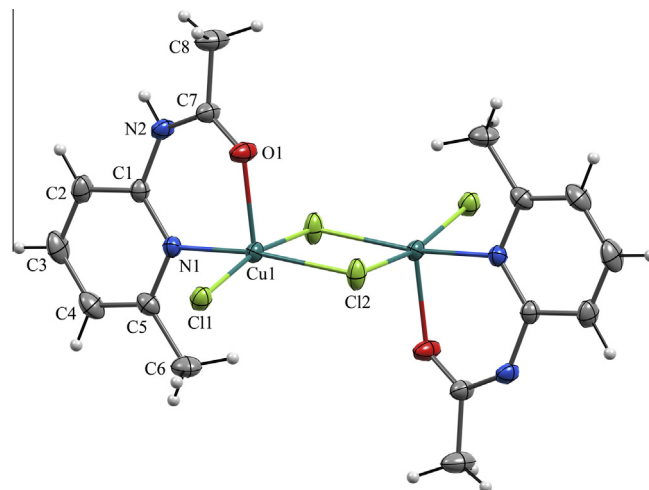**Fig. 1.** Thermal ellipsoid representation (at the 30% probability level) of the binuclear complex [Cu$_2$L$_2$Cl$_4$]. Only the asymmetric unit is numbered. Unnumbered atoms are related to numbered ones by an inversion center midway between the bridging chloride ligands.

hydrogen bonds of 3.29 Å in such a way as to give infinite one-dimensional ribbons parallel to the *a* axis (Fig. 2). Only non-bridging chloride ligands are involved in hydrogen bonding. The ribbons are packed in the crystal lattice without any significant interactions between them other than van der Waals forces.

The compound **1a** crystallizes in the monoclinic space group *P*2$_1$/*n* with 4 formula units per unit cell. All atoms comprising the asymmetric unit, [CuL(H$_2$O)Cl$_2$] neutral complex and uncoordinated L molecule, are located in general positions. The coordination environment of the Cu^{2+} ion in the [CuL(H$_2$O)Cl$_2$] complex includes N and O atoms of the bidentate ligand L, two chloride ions, and O atom of the water molecule. It can be described as either a distorted trigonal bipyramid with the equatorial plane defined by O(1), Cl(1), and Cl(2) atoms, or as a distorted tetragonal pyramid with the basal plane defined by N(1), O(1W), Cl(1), and Cl(2) atoms (Fig. 3). The latter representation is more appropriate since the Cl–Cu–Cl angle is rather wide, 157.54(4)°, while both O$_w$–Cu–Cl angles are close to 90° (Table 3). The Cu–N, Cu–O, Cu–O$_w$ and two Cu–Cl bond lengths are 2.006(3), 2.112(2), 1.957(3), and 2.3629(10) and 2.2794(10) Å, respectively, which are in good agreement with the
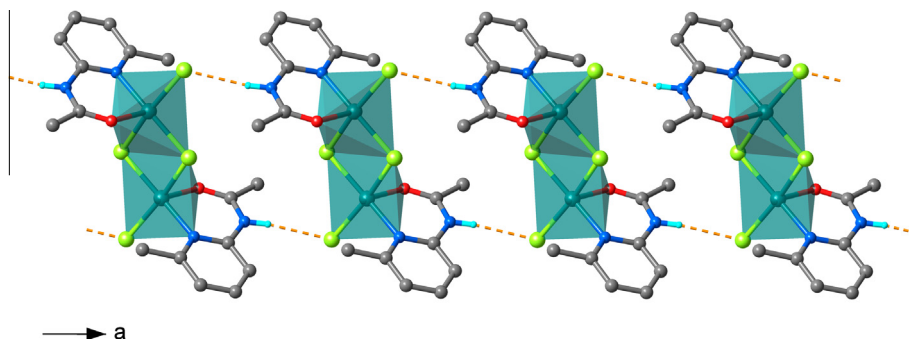
Fig. 2. Fragment of the one-dimensional ribbon along the *a* axis, generated by N_{amide}–H···Cl hydrogen bonds (dashed lines) between the [$Cu_2L_2Cl_4$] molecules in the structure of **1**. For clarity, only those H atoms engaged in hydrogen bonding are shown.

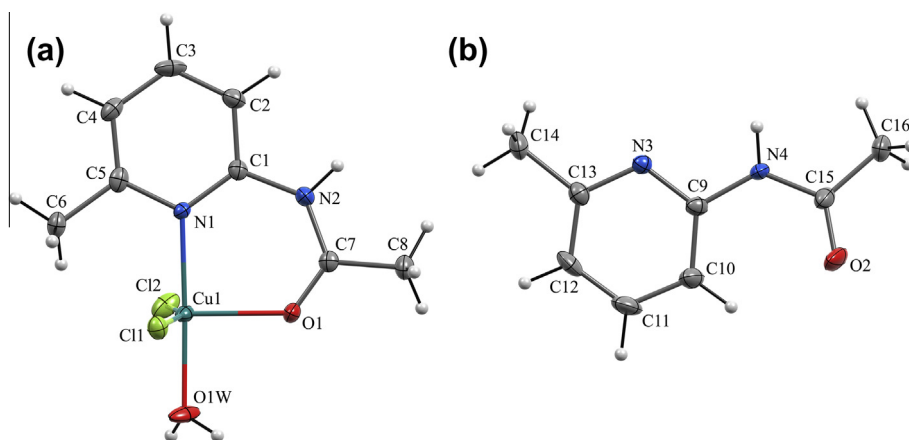**Fig. 3.** Thermal ellipsoid representation (at the 50% probability level) with the atom labeling scheme for (a) [$CuL(H_2O)Cl_2$] complex and (b) uncomplexed L molecule in **1a**.

values typical of the Cu(II) complexes of similar composition. The interesting feature of **1a** is the presence of extra L molecule, which is not involved in coordination to the metal ion and has a somewhat different geometry as compared to the coordinated one. Specifically, it has the acetylamino group rotated by almost 180° with respect to the parent pyridine ring. The C–N_{amide}–C angle in uncoordinated L molecule is expectedly lower, being 128.6(3)° *versus* 131.8(3)° in the coordinated one. Other angles in the acetylamino group are also slightly lower in the case of uncoordinated ligand. In the structure, the [$CuL(H_2O)Cl_2$] complexes are connected in the chains along the *a* axis through the N_{amide}–H···Cl hydrogen bonds of 3.32 Å in length (hereafter the D···A distances are given). Besides, each [$CuL(H_2O)Cl_2$] unit form O_w–H···$N_{pyridine}$, O_w–H···O and weak N_{amide}–H···Cl hydrogen bonds (2.83, 2.71 and 3.51 Å, respectively) with two uncoordinated L molecules through which the adjacent chains are extended into a layer parallel to the *ac* plane (Fig. 4). Only one of two available chloride ligands, Cl(1), is involved in hydrogen bonding. In total, each [$CuL(H_2O)Cl_2$] complex forms five hydrogen bonds. Moreover, the pyridine rings of the adjacent [$CuL(H_2O)Cl_2$] complexes are partially overlapped due to the π-stacking interactions with an interplanar distance of about 3.2 Å.

The compound **2** crystallizes in the monoclinic system with the space group $P2_1/c$ and 4 formula units per unit cell. The asymmetric unit contains the full formula unit. All atoms are in general positions. The structure of **2** is characterized by the simultaneous presence of both possible for Cu^{2+} ion five-coordinate geometries, a distorted trigonal bipyramid and a tetragonal pyramid (Fig. 5). The first one is achieved through the coordination of two bidentate L ligands and one chloride ligand to Cu(1) center, giving the com-

plex cation [CuL_2Cl]$^+$. The second geometry is formed around the Cu(2) center by one coordinated L molecule and three chloride ligands, yielding the complex anion [$CuLCl_3$]$^-$. The Cu–N and Cu–O bond lengths fall in the intervals 2.015(2)–2.029(3) and 2.051(2)–2.158(2) Å, respectively. It is seen that the Cu–O distances are noticeably (up to ∼0.1 Å) shorter in the case of trigonal–bipyramidal coordination, while the Cu–N distances are almost the same in both cases. Comparison of the bond angles in the copper metallocycles indicates that the L molecule is more strained in the case of tetragonal–pyramidal geometry. Particularly, transition from the [$CuLCl_3$]$^-$ anion to the [CuL_2Cl]$^+$ cation is accompanied by the decrease of the C–N_{amide}–C angle from 131.2(3)° to 128.3(3)° and 129.7(3)°. The latter values are comparable with 128.6(3)° observed in free L molecule in **1a**. The Cu–Cl bond lengths vary in the wide range 2.2448(11)–2.3755(10) Å, showing no dependency on the coordination geometry. Summarizing, it is worth to note that for many copper(II) halide complexes with unidentate substituted pyridine-based ligands the same steric influence of the α-substituents is well documented, which, in most cases, makes it impossible for the Cu^{2+} ions to achieve coordination numbers higher than 4 (square-planar coordination) [15–17].

An analysis of the structure of **2** reveals a crucial role of the amide H atoms and chloride ligands in the hydrogen bond formation, similar to that in the above described structures of **1** and **1a**. In particular, the [$CuLCl_3$]$^-$ anions are connected in chains along the *a* axis *via* the N_{amide}–H···Cl hydrogen bonds of 3.37 Å in length. To each member of these chains, the [CuL_2Cl]$^+$ cation is attached through the N_{amide}–H···Cl hydrogen bond of 3.25 Å. Using the other amide H atom, the [CuL_2Cl]$^+$ cation forms strong N_{amide}–H···O hydrogen bond of 2.78 Å with the lattice ethanol molecule,
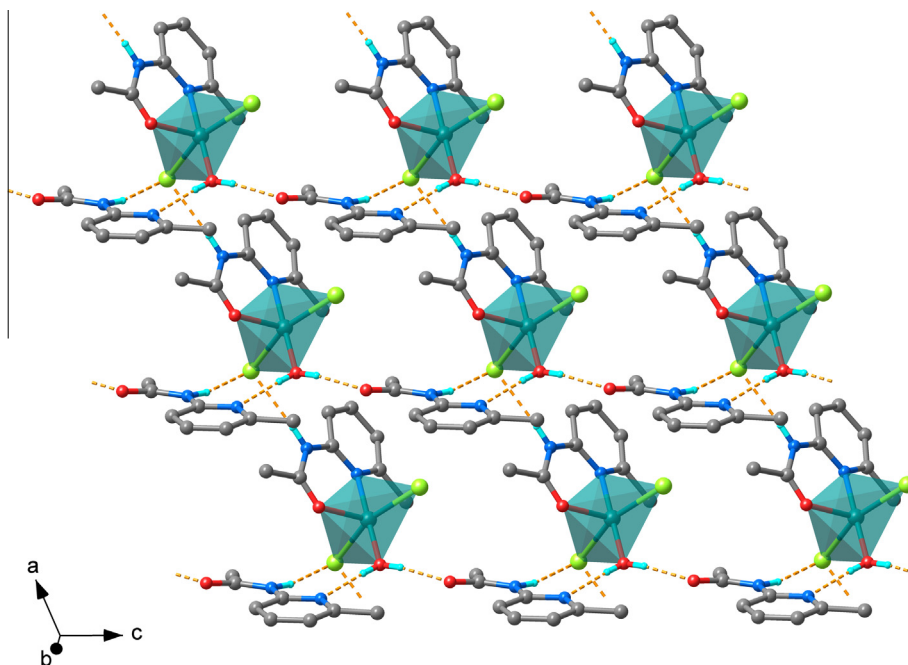
Fig. 4. Fragment of the two-dimensional layer parallel to the *ac* plane in the structure of **1a**, showing $O_w–H \cdots N_{pyridine}$, $O_w–H \cdots O$ and $N_{amide}–H \cdots Cl$ hydrogen bonds (dashed lines) between the $[CuL(H_2O)Cl_2]$ and L molecules. For clarity, only those H atoms engaged in hydrogen bonding are shown.
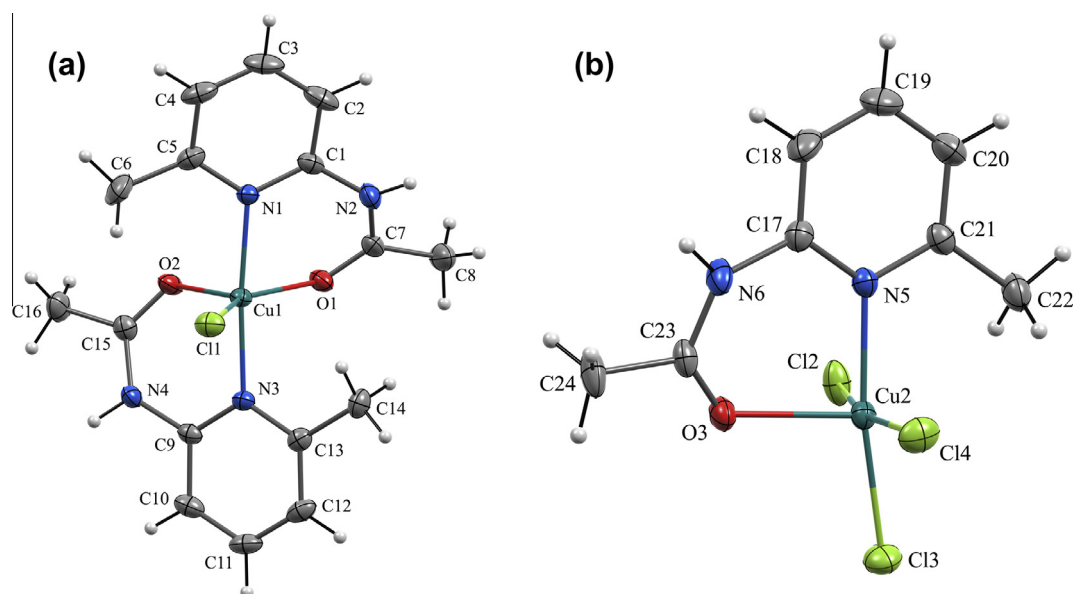

Fig. 5. Thermal ellipsoid representation (at the 30% probability level) with the atom labeling scheme for (a) $[CuL_2Cl]^+$ cation and (b) $[CuLCl_3]^-$ anion in **2**.

whereby the joining of the chains into a layer parallel to the *ab* plane is achieved (Fig. 6). The layers are further interconnected through the π–π interactions between the pyridine rings with interplanar distances ranging from about 3.3 to 3.8 Å.

3.3. IR spectroscopy

It is well-known that the amide group of the ligand L can form intermolecular hydrogen bonds of two types: $N_{amide}–H \cdots N_{pyridine}$ and $N_{amide}–H \cdots O = C$. According to [18,19] only hydrogen bonds $NH \cdots OC$ are realized in 2-(N-acetylamino)-6-methylpyridine; in this case the band in the range 1660 cm^{-1} corresponds to the

vibrations *v*(CO), which are observed in the IR spectrum of L [4]. Amide group, along with the stretching-bending vibrations of the heterocyclic ring, contributes to the intensive absorption bands at 1598, 1582, and 1545 cm^{-1}. The vibrations of NH-groups involved in hydrogen bonding are observed as a wide structured band in the range 3240–3100 cm^{-1}, while the *v*(CH) bands are observed in the range 3050–2780 cm^{-1}.

In the spectra of complexes **1** and **2**, the *v*(NH) bands are shifted (as compared to the spectrum of free L) to higher wavenumbers (3313–3170 cm^{-1}), which obviously can be attributed to the changing of the hydrogen bond pattern. In addition, the effect of ligand coordination and changes in the hydrogen bond network
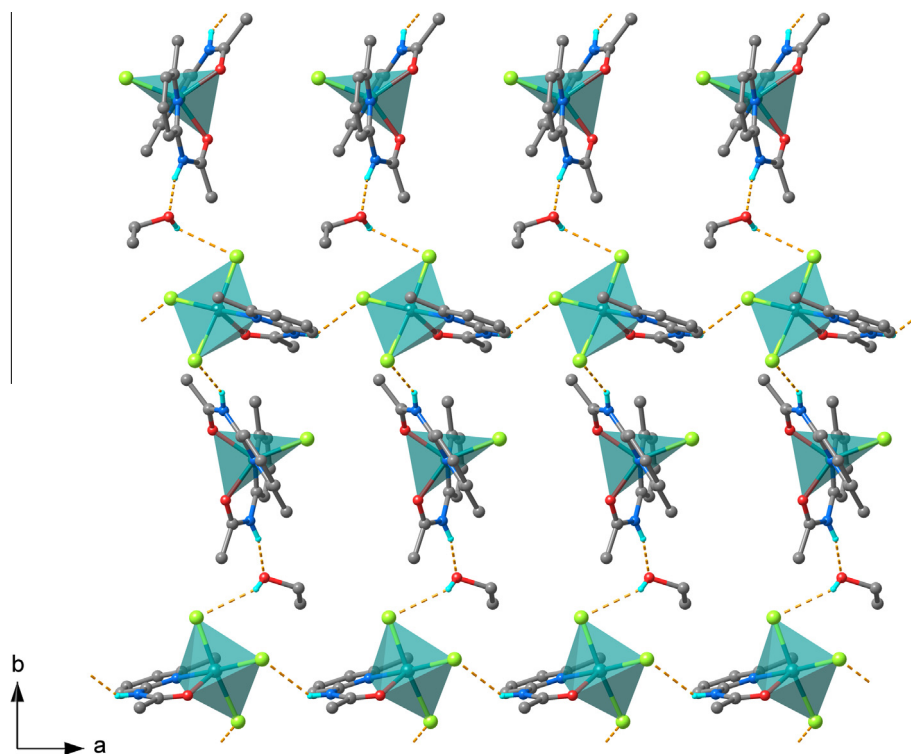
Fig. 6. Projection along the c axis of the two-dimensional layer in the structure of **2**, showing O–H⋯Cl, N_{amide}–H⋯O and N_{amide}–H⋯Cl hydrogen bonds (dashed lines) between the $[CuL_2Cl]^+$ cations, $[CuLCl_3]^-$ anions and solvate ethanol molecules. For clarity, only the H atoms involved in hydrogen bonding are shown.

in **1** and **2** are reflected in the range 1660–1540 cm^{-1}. Particularly, the ν(CO) band appears as split into two components, 1682 and 1619 cm^{-1} for **1**, and 1684 and 1623 cm^{-1} for **2**. The vibrations of the ring are shifted to the values 1536, and 1577 and 1536 cm^{-1} for **1** and **2**, respectively. These facts confirm that pyridine N atom and carbonyl O atom of L are involved in coordination to the Cu(II) ion.

The comparison of the spectra of **1** and **2** with the spectrum of L in the low-frequency regions makes it possible to attribute the bands at 376 (for **1**) and 374 cm^{-1} (for **2**) to the ν(Cu–O) vibrations. The presence of Cu–Cl bonds of different lengths are observed in the spectra as wide bands at 284 (for **1**) and 274 cm^{-1} (for **2**), which correlate with the literature data [20]. The bands at 263 and 257 cm^{-1} correspond to the vibrations ν(Cu–N).

3.4. Magnetic properties of **1**

The temperature plot of μ_{eff} for compound **1** is shown in Fig. 7. In the room-temperature region, the value of μ_{eff} is 2.69 μ_B and remains almost constant up to 50 K. Below 50 K the μ_{eff} value decreases, reaching 0.54 μ_B at 5 K. The room-temperature values of μ_{eff} are slightly higher than the theoretical value of 2.45 μ_B for two almost non-interacting Cu^{2+} ions with the g-factor 2. As the temperature is lowered, the μ_{eff} values decrease, which indicates the predominant antiferromagnetic exchange interactions in **1**. The observed magnetic behavior is typical of compounds whose exchange clusters consist of even number of the paramagnetic centers with identical spin. In the case of **1**, according to the chemical analysis and X-ray diffraction data, the cluster is a dimer, the exchange channel of which is formed by two bridging Cl$^-$ ions.

The optimal values of the effective g-factor and the exchange parameter J/k were found to be 2.220(±0.003) and −12.9(±0.1) K, respectively. The theoretical curve $\mu_{eff}(T)$ corresponding to these values is shown in Fig. 7 by solid line.

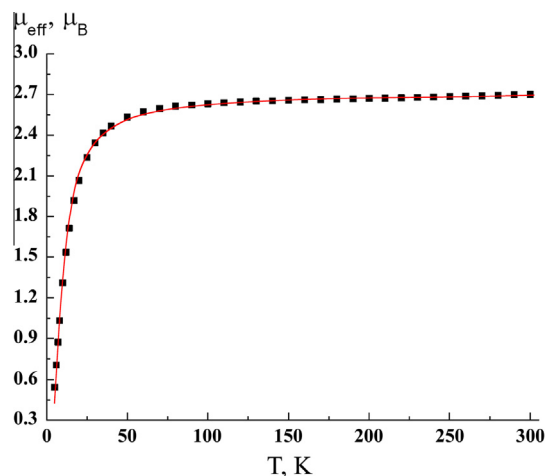**Fig. 7.** Temperature dependence of the μ_{eff} for **1**. Solid line corresponds to the theoretical approximation.

4. Conclusion

In the present work three new complexes of Cu(II) chloride with 2-(N-acetylamino)-6-methylpyridine have been isolated and characterized. The crystal structures of the compounds revealed an important role of the N_{amide}–H⋯Cl intermolecular hydrogen bonds, which force the structural units to organize in one- and two-dimensional associates. The steric hindrance of the 6-methyl group presumably precludes the formation of the octahedral complexes of the type trans-$[CuL_2Cl_2]$ previously reported for unsubstituted 2-(N-acetylamino)pyridine and its 4-methyl derivative. Instead, the Cu^{2+} ion in the title complexes takes either a distorted square-pyramidal or a distorted trigonal–bipyramidal coordination

geometry. It was demonstrated that copper(II) chloride complexes with L exhibiting the Cu:L ratios other than 1:1 and 2:3 could not be prepared. The observations from this work can be used to design new coordination compounds having solid-state organization adjusted in a predictable way through the artful use of steric effects.

Acknowledgments

Appendix Supplementary. data

Crystallographic data for the structures of the compounds **1**, **1a** and **2** have been deposited at the Cambridge Crystallographic Data Center under reference numbers CCDC 987921, 987922, 987923, respectively. Copies of this information may be obtained free of charge from the CCDC, 12 Union Road, Cambridge, CB2 1 EZ, UK (fax: +44-1223-336033; http://www.ccdc.cam.ac.uk/conts/retrieving.html).

References

[1] C. Li, L.S. Rittmann, A.S. Tsiftsoglou, K.K. Bhargava, A.C. Sartorelli, J. Med. Chem. 21 (1978) 874.
[2] W.-H. Sun, W. Zhang, T. Gao, X. Tang, L. Chen, Y. Li, X. Jin, J. Organometal. Chem. 689 (2004) 917.
[3] G.K.-Y. Ng, J.W. Ziller, A.S. Borovik, Inorg. Chem. 50 (2011) 7922.
[4] B. Ośmiałowski, E. Kolehmainen, R. Dobosz, R. Gawinecki, R. Kauppinen, A. Valkonen, J. Koivukorpi, K. Rissanen, J. Phys. Chem. A 114 (2010) 10421.
[5] M. Nonoyama, S. Tomita, K. Yamasaki, Inorg. Chim. Acta 12 (1975) 33.
[6] N. Rajasekar, S. Soundararajan, Curr. Sci. 49 (1980) 886.
[7] V. Scheller-Krattiger, K.H. Scheller, E. Sinn, R.B. Martin, Inorg. Chim. Acta 60 (1982) 45.
[8] G.A. Van Albada, I. Dominicus, I. Mutikainen, U. Turpeinen, J. Reedijk, Polyhedron 26 (2007) 3731.
[9] J.R. Lechat, R.H.P. Francisco, C. Airoldi, Acta Crystallogr., Sect. B 36 (1980) 930.
[10] W. Zhang, X. Leng, W.-H. Sun, J. Chem. Res. 2003 (2003) 808.
[11] H. Kitamura, T. Ozawa, K. Jitsukawa, H. Masuda, Y. Aoyama, H. Einaga, Inorg. Chem. 39 (2000) 3294.
[12] L.V. Sudha, S. Manogaran, D.N. Sathyanarayana, J. Mol. Struct. 129 (1985) 137.
[13] Bruker AXS Inc., APEX2 (Version 1.08), SAINT (Version 7.03), SADABS (Version 2.11), SHELXTL (Version 6.12), Bruker Advanced X-ray Solutions, Madison, WI, USA, 2004.
[14] K. Brandenburg, H. Putz, DIAMOND (Version 3.2g), Crystal Impact GbR, Bonn, Germany, 2011.
[15] V.F. Duckworth, N.C. Stephenson, Acta Crystallogr., Sect. B 25 (1969) 1795.
[16] W. Stählin, H.R. Oswald, Acta Crystallogr., Sect. B 27 (1971) 1368.
[17] J.A. Campbell, C.L. Raston, J.N. Varghese, A.H. White, Aust. J. Chem. 30 (1977) 1947.
[18] E. Fan, J. Yang, S.J. Geib, T.C. Stoner, M.D. Hopkins, A.D. Hamilton, J. Chem. Soc., Chem. Commun. (1995) 1251.
[19] F. Garcia-Tellado, S.J. Geib, S. Goswami, A.D. Hamilton, J. Am. Chem. Soc. 113 (1991) 9265.
[20] L.V. Stepakova, M.Yu. Skripkin, L.V. Chernykh, G.L. Starova, L. Hajba, J. Mink, M. Sandström, J. Raman Spectrosc. 39 (2008) 16.